Aurora A phosphorylates Ndel1 to reduce the levels of Mad1 and NuMA at spindle poles

Paweł Ł. Janczyk[a,b], Eliza Żyłkiewicz[a,†], Henry De Hoyos[a], Thomas West[a,‡], Daniel R. Matson[a,§], Won-Chan Choi[c,ǁ], Heather M. Raimer Young[a], Zygmunt S. Derewenda[c], and P. Todd Stukenberg[a,*]

[a]Department of Biochemistry and Molecular Genetics, [b]Department of Pathology, and [c]Department of Molecular Physiology and Biological Physics, University of Virginia School of Medicine, Charlottesville, VA 22903

ABSTRACT Dynein inactivates the spindle assembly checkpoint (SAC) by transporting checkpoint proteins away from kinetochores toward spindle poles in a process known as "stripping." We find that inhibition of Aurora A kinase, which is localized to spindle poles, enables the accumulation of the spindle checkpoint activator Mad1 at poles where it is normally absent. Aurora kinases phosphorylate the dynein activator NudE neurodevelopment protein 1 like 1 (Ndel1) on Ser285 and Mad1 accumulates at poles when Ndel1 is replaced by a nonphosphorylatable mutant in human cells. The pole focusing protein NuMA, transported to poles by dynein, also accumulates at poles in cells harboring a mutant Ndel1. Phosphorylation of Ndel1 on Ser285 is required for robust spindle checkpoint activity and regulates the poles of asters in *Xenopus* extracts. Our data suggest that dynein/SAC complexes that are generated at kinetochores and then transported directionally toward poles on microtubules are inhibited by Aurora A before they reach spindle poles. These data suggest that Aurora A generates a spatial signal at spindle poles that controls dynein transport and spindle function.

INTRODUCTION

The formation of a mitotic spindle requires both spatial and temporal regulation to ensure accurate segregation of chromosomes. A major form of temporal regulation is generated by the spindle assembly checkpoint (SAC), which controls the cell cycle to ensure that all chromosomes have aligned at the metaphase plate before the cell segregates sister chromatids at anaphase. It has been suggested that Aurora kinases are a source of spatial information because they localize to distinct locations on the mitotic spindle, including Aurora A kinase that is found at spindle poles (Giet and Prigent, 2000; Giet *et al.*, 2002; Carmena and Earnshaw, 2003; Barr and Gergely, 2007).

Cytoplasmic dynein 1 (dynein) is the major minus end directed microtubule motor. The loading and unloading of dynein onto microtubules, and the interaction of dynein with its cargo, must be tightly regulated to carry out dynein's numerous cellular functions. However, the mechanisms that disassemble dynein complexes on microtubules are poorly understood. During formation of the mitotic spindle, dynein transports proteins such as nuclear mitotic apparatus protein 1 (NuMA) that cross-link microtubules to spindle poles (Vaisberg *et al.*, 1993; Heald *et al.*, 1996; Merdes *et al.*, 2000). Moreover, as kinetochore–microtubule attachments are formed and chromosomes align at the metaphase plate, dynein removes the SAC proteins from kinetochores in a process known as "dynein stripping" (King *et al.*, 2000; Howell *et al.*, 2001). After dynein strips SAC proteins off kinetochores, they do not accumulate at poles, indicating that there may be mechanisms that limit dynein transport on the spindle. The strongest data for this model comes from a classic experiment where cellular ATP levels were decreased and both dynein and the SAC proteins accumulate at poles (Howell *et al.*, 2001). This

classic experiment suggests that low ATP levels are sufficient for dynein motility but there are ATP-dependent mechanisms that prevent dynein from carrying cargo the full distance to spindle poles.

Dynein processivity is tightly regulated via interactions with accessory proteins including NudE neurodevelopment protein 1 like 1 (Ndel1) and lissencephaly-1 (Lis1; Reck-Peterson et al., 2018). Ndel1 forms a homodimer through a long coiled-coil domain, which acts as a regulated molecular scaffold to link dynein to its processivity factor Lis1 (Efimov and Morris, 2000; Derewenda et al., 2007; McKenney et al., 2010; Wang and Zheng, 2011; Żyłkiewicz et al., 2011; Huang et al., 2012). Interactions between Ndel1, Lis1, and dynein are regulated by phosphorylation of the C-terminal unstructured domain of Ndel1 (Mori et al., 2007; Hebbar et al., 2008; Bradshaw et al., 2011; Żyłkiewicz et al., 2011). This region is phosphorylated on at least seven sites by four kinases, supporting a complex pattern of regulation (Mori et al., 2007; Hebbar et al., 2008; Bradshaw et al., 2011; Żyłkiewicz et al., 2011; Takitoh et al., 2012; Wynne and Vallee, 2018). The C terminus of Ndel1 also contains a short helix that binds the dynein regulator disrupted in schizophrenia 1 (DISC1; Kamiya et al., 2006; Ye et al., 2017).

Aurora A kinase is found at spindle poles after nuclear envelope breakdown (Gopalan et al., 1997; Giet and Prigent, 2000; Katayama et al., 2008; Chmátal et al., 2015; DeLuca et al., 2018b; Eot-Houllier et al., 2018). Aurora A is required for proper pole formation and most likely phosphorylates many sites to do this. One key substrate is the NuMA protein that is transported by dynein to poles. Once at poles, NuMA cross-links microtubules to generate a focus of microtubule minus ends (Gaglio et al., 1995; Merdes et al., 1996; Dionne et al., 1999; Silk et al., 2009; Seldin et al., 2016; Chinen et al., 2020). Ndel1 is phosphorylated by Aurora A on Ser251 during prophase, which is required for transforming acidic coiled-coil (TACC) recruitment to stabilize spindle poles (Mori et al., 2007, 2009; Takitoh et al., 2012), but this phospho-epitope is not detected during later stages of mitosis.

The localization of Aurora A kinase to poles provides a potential mechanism to generate spatial information that defines a location on the mitotic spindle. Dynein stripping provides an experimental opportunity to test this idea because the complexes are generated at kinetochores and then directionally transported toward the poles. Here we identify a mechanism that limits dynein/SAC protein complexes before they reach spindle poles. We show that Aurora A can directly phosphorylate Ndel1 at S285 in vitro. Nonphosphorylatable mutants of Ndel1 accumulate the dynein cargoes NuMA and Mad1 at poles suggesting a role in down-regulating dynein activity. Phosphorylation of Ndel1 on Ser285 is also required to maintain a robust SAC response. Phosphorylation of Ndel1 by Aurora is required for pole formation during Xenopus aster formation assays, which mimics pole formation in the absence of redundant activities from centrosomes. Our findings suggest Aurora A phosphorylates Ndel1 on transporting dynein complexes as they near the poles to limit the accumulation of NuMA and release SAC proteins before they reach spindle poles. These data provide a mechanism to regulate dynein transport and a formal test that Aurora A at poles can generate spatial cues to control the mitotic spindle.

RESULTS
Mad1 accumulates at spindle poles after inhibition of Aurora A kinase activity
We observed that the SAC protein Mad1 localized to poles in a dose-dependent manner after treatment with the pan Aurora kinase inhibitor VX680 (Supplemental Figure S1, A–C; Harrington et al., 2004). The IC50 of VX680 for Aurora A is only threefold lower than

Aurora B kinase (de Groot et al., 2015). We then employed two specific Aurora inhibitors that have distinct structures from VX680 to determine which of the Aurora kinases was responsible for this effect. Aurora A inhibition by MLN8054 (MLN) but not Aurora B by AZD1152 resulted in an accumulation of Mad1 at the spindle poles. MLN8054 (200 nM) produced a statistically significant increase in Mad1 at poles and strongly inhibited T-loop autophosphorylation on Aurora A but had little effect on Aurora B (Figure 1, A–D, and Supplemental Figure S1, D–I). Both MLN and AZD reduced the amount of Mad1 at kinetochores, consistent with previous results that demonstrate Aurora B regulates Mad2 levels at the kinetochores (Figures 1, A–D, and Supplemental Figure S1, D–I; Ditchfield et al., 2003; Matson and Stukenberg, 2014). These data suggest that Aurora A activity near spindles promotes the release of stripped SAC proteins before they reach the poles.

We confirmed that this accumulation of Mad1 at poles was dynein dependent by treating HeLa cells with Aurora A inhibitors while also expressing either GFP or the GFP-CC1, which is a dominant negative fragment of the dynactin complex (Quintyne et al., 1999). We found that Mad1 failed to accumulate at the spindle poles if both Aurora A and dynein activity was inhibited, indicating that the pole accumulation of Mad1 at poles is dynein dependent (Figure 1E and quantified in Figure 1F).

Aurora kinases phosphorylate Ndel1 near a C-terminal helix at kinetochores and spindle poles
Phosphoregulation of dynein is often mediated by its regulator Ndel1. Ndel1 has an N-terminal coiled coil that acts as a regulated molecular scaffold to link dynein to its processivity factor Lis1 (Efimov and Morris, 2000; McKenney et al., 2010; Żyłkiewicz et al., 2011; Huang et al., 2012). Ndel1 is regulated by multiple phosphorylation sites on its C-terminal unstructured domain (Mori et al., 2007; Hebbar et al., 2008; Bradshaw et al., 2011; Żyłkiewicz et al., 2011; Takitoh et al., 2012; Wynne and Vallee, 2018), and we hypothesized that Aurora kinase phosphorylates Ndel1 (Figure 2A and Supplemental Figure S2A) to regulate dynein stripping. Different fragments of recombinant mouse Ndel1 (mNdel1) protein were phosphorylated by Aurora A and Aurora B kinases in vitro (Figure 2B and Supplemental Figure S2B). Two Ndel1 fragments that contain portions of the C-terminal tail, mNdel1$^{191–250}$ and mNdel1$^{8–310}$, were in vitro substrates of both Aurora A and Aurora B (Figure 2B). Next, we mapped these in vitro phosphorylation sites by mass spectrometry on the mNdel1$^{8–310}$ protein, and identified a previously unknown phosphorylation site on Ser285 that fits the Aurora kinase consensus sequence (Supplemental Figure S2C). Interestingly, this site sits next to a helix that binds the DISC1 protein (Ye et al., 2017), which is also required for dynein function, and a previously characterized Aurora phosphorylation site sits on the other end of this helix (S251). We performed in vitro kinase assays with Aurora A and Aurora B on recombinant mNdel1$^{8–310}$ containing alanine substitutions at Ser194 (which fits the Aurora consensus), Ser285, or Ser251 (Figure 2C). Both Aurora kinases poorly phosphorylated the Ndel1 S285A mutant but phosphorylation of the Ser194A or S251A mutant were not dramatically affected (Figure 2C). We conclude that Ser285 is a major Aurora kinase in vitro phosphorylation site in the C terminus of Ndel1.

To determine the mitotic subcellular location where Ndel1 is phosphorylated on Ser285, we raised polyclonal rabbit antibodies against a peptide containing the 15 amino acids that surround Xenopus Ser285 with phosphorylated serine Ser285 in the central position. Antibodies were passed through a column containing an unmodified peptide, and subsequently affinity purified using the
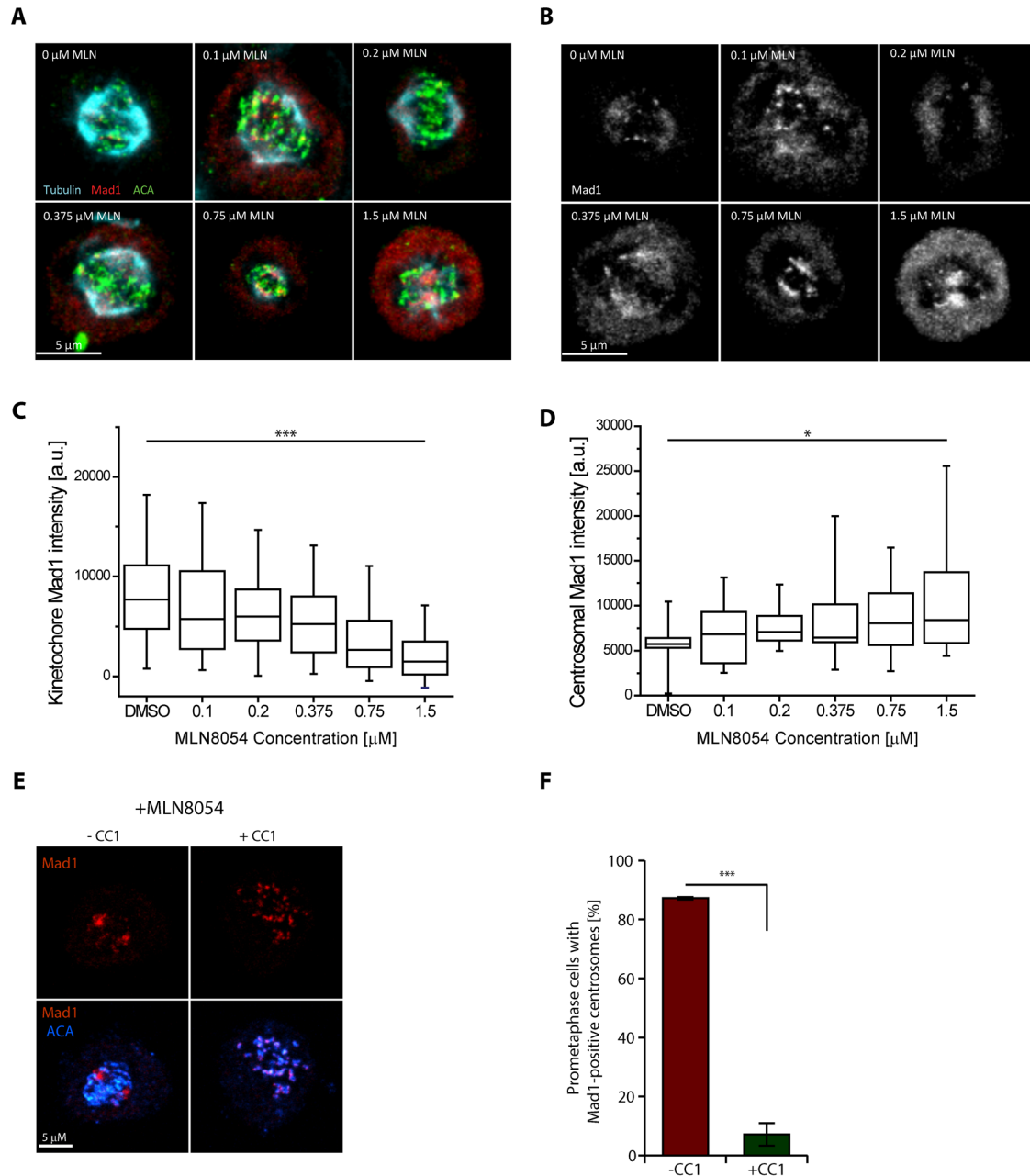
FIGURE 1: The Mad1 SAC protein relocalizes from kinetochores to spindle poles after inhibition of Aurora A kinase activity in prometaphase cells. (A, B) Representative images depicting the localization of Mad1 (red) in HeLa T-Rex cells treated with increasing concentrations of Aurora A inhibitor MLN8054, with tubulin (cyan) and centromere (green) costaining. Note: Aurora A inhibition by MLN had an unexpected effect on anti-centromere antigen (ACA) staining so we altered the levels of ACA in each image so that centromeres are clearly visible. The ACA staining has not been adjusted in Supplemental Figure S1. Bar = 5 µm; $N = 3$ experimental repeats. (C, D) Quantification of Mad1 fluorescent intensity at the kinetochores (C) and at the spindle poles (D) in the experiment depicted in panels A and B. We have not ratioed the Mad1 staining by the ACA signal; however, we confirmed that the results were similar if this was done (Supplemental Figure S1). (Box, 25th–75th percentile; whisker, 5th–95th percentile; bar in middle, median. One-way ANOVA, with *, $p < 0.05$; ***, $p < 0.0005$. (E) Representative images depicting localization of Mad1 (red) in HeLa T-Rex cells expressing GFP (−CC1) or GFP-CC1 (+CC1) in mitotic cells treated with 1.5 µM MLN8054; bar = 5 µm. (F) Quantification of cells containing visible Mad1 signal at centrosomes from experiment depicted in panel C ($n > 100$ cells; $N = 3$; ***, $p < 0.005$; Student's t test, unpaired).

target pSer285 phosphopeptide. We then analyzed the localization of Ndel1 pSer285 in mitotic *Xenopus* S3 cells (a nontransformed cell line that remains flat during mitosis with large spindles) by immunofluorescence. Both Ndel1 (Figure 2D) and Ndel1 pS285 signals colocalize with Ndc80 at most kinetochores in prometaphase and some but not all kinetochores in metaphase (Figure 2E). Ndel1 Ser285 phosphorylation also strongly labeled centrosomes, and this was was dependent on Aurora kinase activity and could be competed by the phosphorylated peptide (Figure 2E and Supplemental Figure S2, D–G). We conclude that Aurora kinases phosphorylate
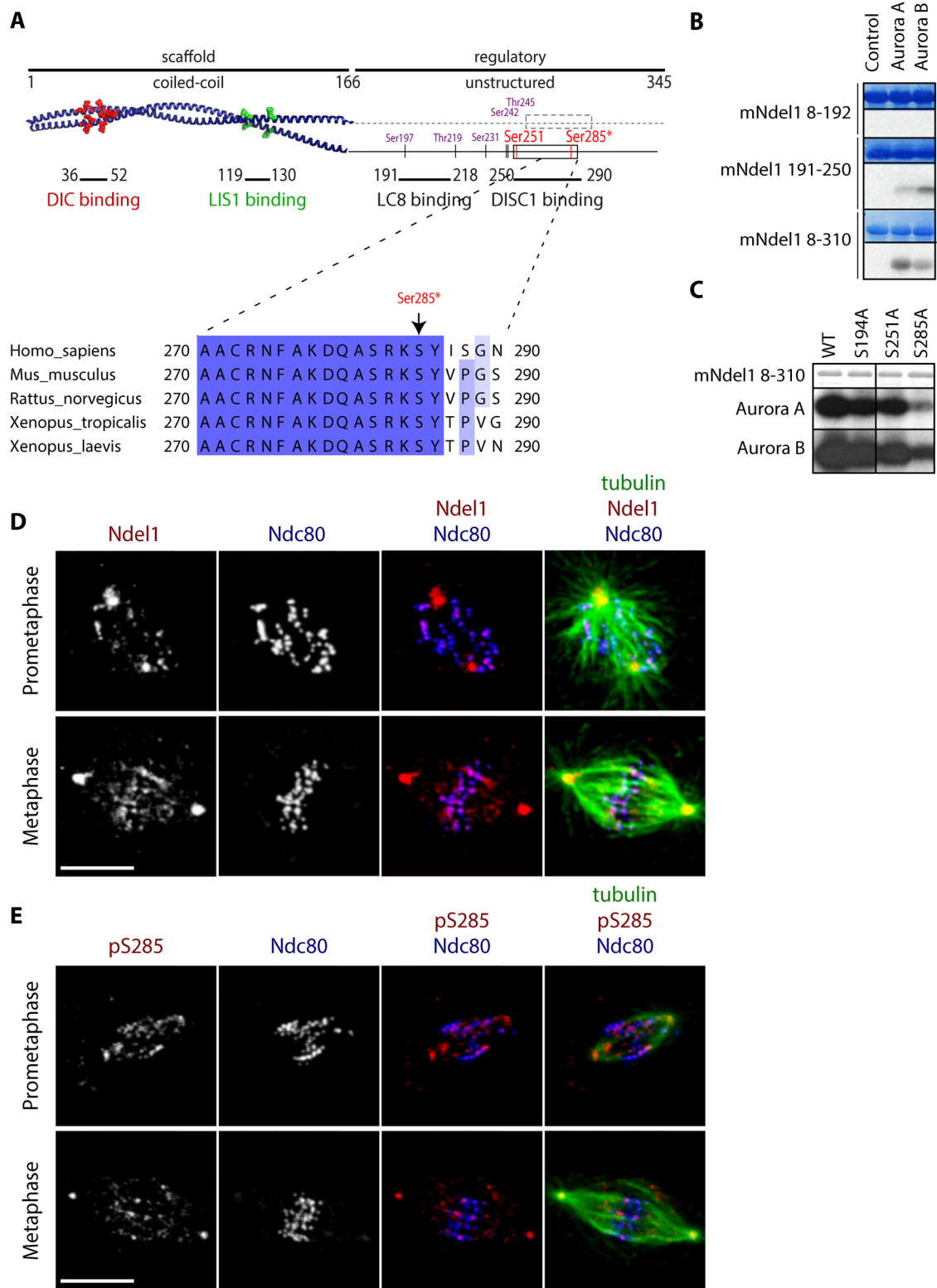
FIGURE 2: Aurora kinases phosphorylate Ndel1 near a C-terminal helix I Ser285 at spindle poles and kinetochores. (A) Domain structure of Ndel1. Crystal structure of the N-terminal coiled-coil domain (PDB: 2V71) with critical amino acids required for dynein intermediate chain (DIC) binding (red ball and stick) and Lis1 (green ball and stick) highlighted. The C terminus of Ndel1 is mostly unstructured but contains two protein binding sites and a number of previously identified phosphorylation sites (purple), including previously reported Aurora site Ser251 (red). Here we describe a new Aurora phosphorylation site Ser285 (red with asterisks). Note that two Aurora sites are conserved in frogs, rodents, and humans and flank an alpha helical domain (box) that is required for DISC1 binding. (B) The C terminus of Ndel1 is phosphorylated by Aurora kinases. The indicated mNdel1 fragments were phosphorylated in vitro by either recombinant Aurora A or Aurora B kinase and analyzed on the SDS–PAGE and autoradiography. (C) Ser285 is the

Ndel1 at Ser285 at spindle poles and the kinetochores of unaligned chromosomes.

Phosphorylation of Ndel1 at S285 prevents accumulation of SAC proteins at poles

To determine whether Ndel1 phosphorylation at S285 underlies the accumulation of Mad1 seen after treatments with Aurora A inhibitors (Figure 1 and Supplemental Figure S1), we visualized mitotic events in human cells after the replacement of the endogenous Ndel1 with either recombinant Nde1-GFP or Ndel1(S285A)-GFP. The siRNA treatment efficiently depleted the endogenous proteins and rescued recombinant proteins were higher than endogenous proteins (Ndel1[S285A]-GFP is also higher than Nde1-GFP; Supplemental Figure S3A). Prometaphase cells expressing the Ndel1 S285A accumulate Mad1 at the spindle poles (Figure 3A and quantified in Figure 3B), suggesting that Aurora phosphorylation of Ndel1 S285 is required to limit dynein-dependent transport of SAC proteins.

To determine whether Aurora phosphorylation of Ndel1 affects SAC signaling, we treated the cells replaced with either Ndel1 wild-type (WT) or Ndel1 S285A mutant with low concentrations of nocodazole and measured SAC arrest. While the nontreated cells did not show any difference in proliferation (Supplemental Figure S3B), the low dose of nocodazole dramatically reduced proliferation of cells replaced with the WT Ndel1 transgene. Interestingly, cells expressing the Ndel1 S285A mutant showed significantly faster proliferation (Figure 3C and Supplemental Figure S3, C and D). The simplest explanation for the increase in proliferation was that cells expressing Ndel S285A escape SAC arrest more often. Cells expressing Ndel1 S285A mutant slipped out of the mitotic arrest generated by nocodazole more efficiently than the cells expressing Ndel1 WT protein as visualized by live-cell imaging, which can in part explain the reduced proliferation of the Ndel1 WT cells (Figure 3D and Supplemental Figure S3, E and F). We conclude that Aurora phosphorylation of Ndel1 is required for robust SAC arrest.

Phosphorylation of Ndel1 on Ser285 also limits the localization of NuMA to spindle poles and negatively regulates dynein-dependent aster formation in *Xenopus* egg extracts

Dynein-dependent transport of NuMA to spindle poles is crucial for spindle pole assembly and maintenance (Merdes *et al.*, 1996, 2000, reviewed in Kiyomitsu and Boerner, 2021). Previous work has shown that Aurora A phosphorylates NuMA to limit that accumulation of NuMA at poles (Gallini *et al.*, 2016). To ascertain whether Ndel1 S285 phosphorylation also regulates the localization of NuMA at poles, we visualized the mitotic event in human cells after the replacement of the endogenous Ndel1 with either recombinant Nde1-GFP or Ndel1(S285A)-GFP. Cells were stained with anti-NuMA, tubulin, and anti-centromere antigen (ACA) antibodies to visualize the localization of NuMA at poles. Ndel1 S285A mutant shows increased accumulation of NuMA at the spindle poles (Figure 4A and quantified in Figure 4B). These results suggest that dynein-dependent accumulation of NuMA is also limited by Aurora phosphorylation of Ndel1 at S285.

To measure a role for Ndel1 phosphorylation in pole formation, we measured Ran-dependent aster formation in the *Xenopus* egg extract system. This reaction is Ndel1, dynein, and NuMA dependent and mimics the formation of spindle poles in the absence of redundant activities supplied by centrosomes (Merdes *et al.*, 1996; Wiese *et al.*, 2001; Zyłkiewicz *et al.*, 2011). Ndel1 was immunodepleted from *Xenopus* egg extracts with polyclonal antibodies that specifically remove Ndel1, but not dynein, dynactin, or Lis1 (Zyłkiewicz *et al.*, 2011). Ndel1 function was rescued by the addition of recombinant mouse Ndel1 proteins at either the measured endogenous concentration (100 nM) or at two lower concentrations (50 and 10 nM). As expected, Ndel1 depletion yielded unfocused microtubule structures consistent with previous reports (Figure 4C and quantified in Figure 4D; Wang and Zheng, 2011; Zyłkiewicz *et al.*, 2011). Adding back endogenous amounts of both the WT and mutant mNdel1[8–310] protein completely rescued this phenotype (Figure 4C and quantified in Figure 4D). However, the WT protein lost its ability to generate asters when we decreased the amount of recombinant protein in rescue experiments to 50% or 10% of endogenous concentration (Figure 4C and quantified in Figure 4D). In contrast, 10% of mNdel1[8–310] S285A fully rescued aster formation (Figure 4C and quantified in Figure 4D), suggesting that Aurora kinase phosphorylation limits Ndel1 function. Next, we performed similar experiments using a phosphomimetic mutant mNdel1[8–310] S285D. At endogenous concentrations and at 50% of the endogenous concentration, mNdel1[8–310] S285D partially rescued aster formation, but not as effectively as the WT protein (Figure 4E and quantified in Figure 4F). At 10% of the endogenous concentration, both proteins almost completely lost the ability to support aster formation, in clear contrast to the mNdel1[8–310] S285A mutant (Figure 4E and quantified in Figure 4F). Thus, the nonphosphorylatable mutant increased dynein activity and the phosphomimetic decreased dynein activity in *Xenopus* aster formation. We conclude that Aurora kinase phosphorylation of S285 down-regulates Ndel1/dynein focusing of spindle poles.

DISCUSSION

Dynein uses its ATPase motor activity to transport SAC proteins away from kinetochores after kinetochores obtain proper "end-on" attachments. It is believed that the SAC signal can only be generated at kinetochores and this transport inactivates the SAC signal and promotes cell cycle progression. However, SAC proteins are not carried by dynein all the way to poles, and the reason for this was poorly understood. We show that Aurora A kinase, which is located near spindle poles, phosphorylates the dynein activator Ndel1 on S285 to prevent accumulation at poles. We inhibited this mechanism both by adding Aurora A small molecule inhibitors and by expressing a nonphosphorylatable Ndel1 site mutant, and both conditions resulted in accumulation of SAC proteins at spindle poles. Phosphorylation may be a general mechanism to inactivate dynein transport, as dynein light chain Tctex-type 1 (Tctex-1) is also phosphorylated to dissociate dynein from its rhodopsin cargo in polarized cells (Yeh *et al.*, 2006).

Our results provide an explanation for a classic result that was used to establish the concept of SAC stripping by dynein (Howell *et al.*, 2001). SAC proteins accumulated at poles if cells were treated

dominant Aurora phosphorylation site on Ndel1. The serines that fit the known Aurora consensus in the C terminus of Ndel1 were mutated to alanines and tested in in vitro kinase assays with Aurora A or Aurora B kinase. (D) Ndel1 (red) signal colocalizes with Ndc80 (blue) at most kinetochores and centrosomes in both prometaphase and metaphase in *Xenopus laevis* S3 cells; bar = 10 μm. (E) Ndel1 pS285 (red) signal colocalizes with Ndc80 (blue) at kinetochores and centrosomes in mitotic *Xenopus laevis* S3 cells; bar = 10 μm.
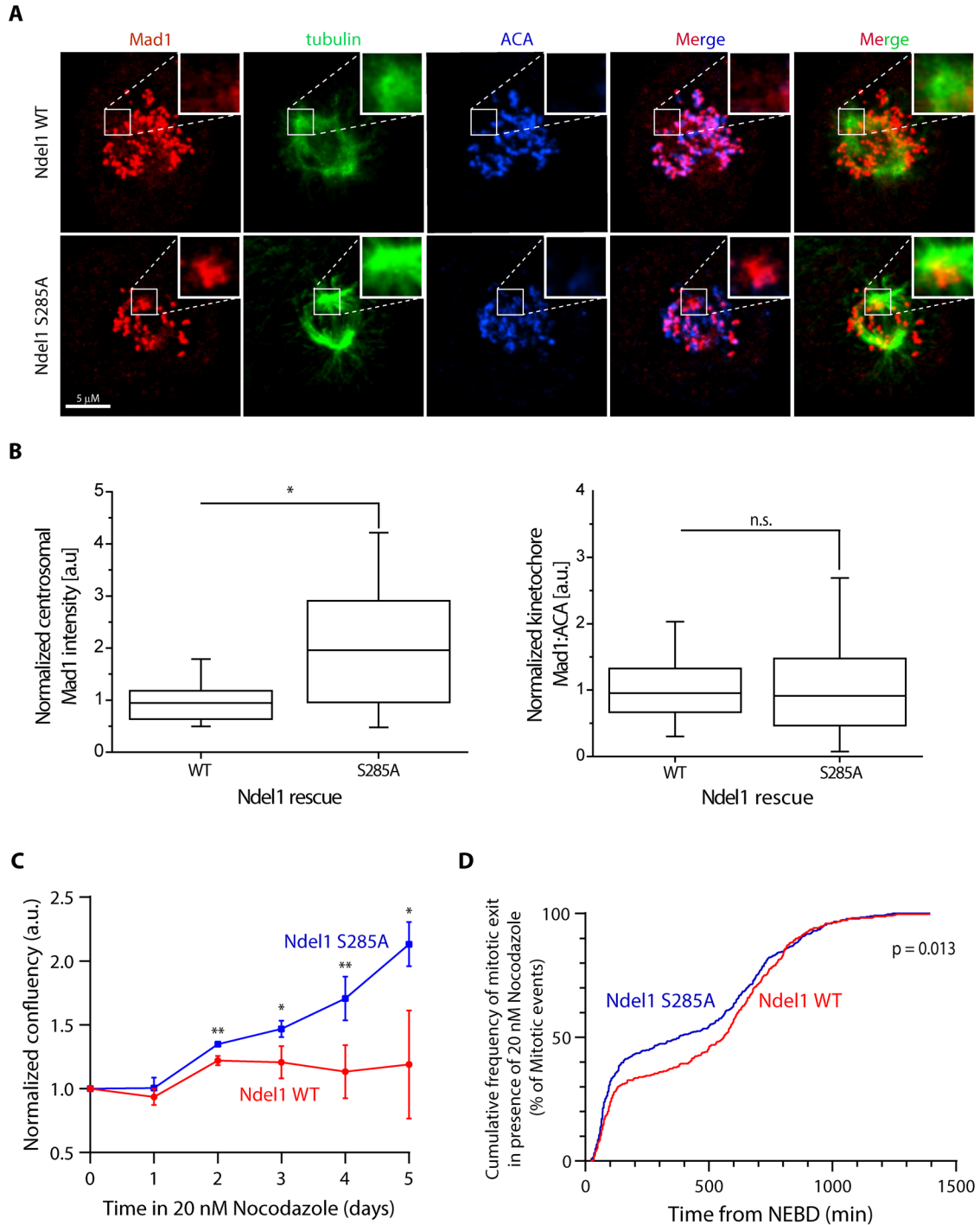
FIGURE 3: Phosphorylation of Ndel1 at S285 regulates dynein stripping and spindle checkpoint function. (A) Representative images depicting localization of Mad1 (red) in HeLa T-Rex cells stably expressing Ndel1 WT or S285A after removal of endogenous Ndel1 by siRNA; bar = 5 μm. Insets represent maximum projection of one to two Z-slices of the centrosomal region. (B) Quantification of Mad1 fluorescent intensity at centrosomes (left graph, $n > 16$ centrosomal regions) or kinetochores (right graph, $n > 300$ kinetochores) from the experiment depicted in panel A. ($N = 3$; *, $p < 0.05$; n.s., $p > 0.05$; Student's t test, unpaired). (C) A nonphosphorylatable mutant of Ndel1 shows increased proliferation rates in the presence of 20 nM nocodazole. Graph depicts confluency normalized to day 0 of HeLa T-Rex cells expressing either Ndel1 WT or Ndel1 S285A mutant grown in the presence of 20 nM nocodazole ($n = 4$; $N = 3$; Student's t test, with *, $p < 0.05$; **, $p < 0.005$). (D) HeLa T-Rex cells expressing either Ndel1 WT or Ndel1 S285A mutant were imaged in the presence of 20 nM nocodazole and 100 nM SiR-DNA for 24 h. Graph represents cumulative frequency of time spent from NEBD until mitotic exit through anaphase or mitotic catastrophy ($n > 130$ cells; $N = 2$; Kolmogorov-Smirnov test).

with NaAzide and deoxyglucose to reduce ATP (Howell *et al.*, 2001). The interpretation being that the treated cells had enough ATP for dynein to walk on microtubules but not enough for an ATP-sensitive factor that prevents accumulation of SAC proteins at poles. Our data suggest that Aurora A kinase is the ATP-sensitive factor that prevents accumulation of SAC proteins at poles. Moreover, Aurora A does this by phosphorylating Ndel1 to limit dynein activity. At this point we do not know whether the phosphorylation of Ndel1 on S285 causes the release of cargo from dynein or triggers the dissociation of dynein from microtubules near the poles but note that dynein accumulated at poles after treatments that reduce ATP (Howell *et al.*, 2001), which is consistent with Aurora A releasing dynein from microtubules. Our experiments also suggest that the release of SAC proteins at poles has a function in cell cycle progression in that nonphosphorylatible mutants of Ndel1 fail to generate a robust SAC response. The simplest explanation is that the release of SAC proteins replenishes a soluble pool of SAC proteins so that they can be recycled onto signaling kinetochores.

Aurora kinases have distinct locations and have been shown to generate gradients of kinase activity (Fuller *et al.*, 2008; Wang *et al.*, 2011; Ye *et al.*, 2015). However, there are limited examples of how cells actually use these gradients to generate spatial information to control mitotic events (Chmátal *et al.*, 2015; Ye *et al.*, 2015; Mangal *et al.*, 2018). We propose a model whereby dynein carries SAC proteins away from kinetochore along microtubules until it reaches a region of high Aurora A kinase activity near spindle poles. At this point, Ndel1 is phosphorylated at S285 to inhibit the transport of SAC proteins by dynein. This is supported by a previous report showing Aurora A limited NuMA accumulation at the spindle pole upon Aurora A inhibition (Gallini *et al.*, 2016).

Our studies have focused on the role of the Ndel1 S285 phosphorylation at poles, and additional studies are required to elucidate the role of S285 phosphorylation at kinetochores. We speculate that an Aurora kinase (likely Aurora B, although Aurora A has been shown to phosphorylate some sites on kinetochores; DeLuca *et al.*, 2018a) can also phosphorylate Ndel1 on S285 to inhibit the initiation of dynein stripping on unaligned chromosomes. However, our experiments to test this idea were not conclusive. We saw no change to the amount of Mad1 at kinetochores in cells expressing the S285A mutant, suggesting that if phosphorylation of S285 plays a role, there are additional mechanisms to prevent stripping. There are many possible regulators such as spindly and CENP-F that could work in combination with Ndel1 phosphorylation to prevent dynein stripping until microtubules are properly attached by kinetochores (Gassmann *et al.*, 2010; Auckland *et al.*, 2020). An interesting possibility is Ndel1 homologue Nde1, which also controls stripping at kinetochores (Auckland *et al.*, 2020) and the Aurora site on S250 is well conserved, while the site at S285 is replaced by a putative CDK1 site. How phosphorylation of S285 controls Ndel1 function is also an important area of future research. Ndel1 S285 and another reported Aurora site S251 are located on two ends of an alpha helix that has been reported to interact with dynein and the dynein regulator DISC1 (Kamiya *et al.*, 2006; Stehman *et al.*, 2007; Wang and Zheng, 2011; Zyłkiewicz *et al.*, 2011; Nyarko *et al.*, 2012; Ye *et al.*, 2017). It will be important to test whether S285 phosphorylation inhibits one of these interactions to inhibit dynein activity.

Previous studies have reported Aurora A also phosphorylates NuMA directly to limit the amount of NuMA at poles (Gallini *et al.*, 2016) where it cross-link spindles microtubules. We have extended this study by showing that Aurora A also phosphorylates Ndel1 to regulate dynein transport of NuMA to poles. Moreover, Ndel1 phosphorylation mutants regulated Ran aster formation, which is a subreaction of spindle pole formation that requires NuMA deposition. Thus, Aurora controls at least two dynein/cargo pairs at spindle poles (dynein/Mad1 and dynein/NuMA) as well as having multiple substrates to limit NuMA deposition (NuMA and Ndel1) to regulate spindle poles.

MATERIALS AND METHODS

Tissue culture

Xenopus S3 cells were cultured at 18°C in 66% L-15 media (Sigma) supplemented with 10% fetal bovine serum (FBS), 1 mM sodium pyruvate, 100 IU/ml penicillin, and 100 µg/ml streptomycin (Invitrogen). Before fixation, cells were grown on acid-washed *poly*-lysine or fibronectin (Sigma) -coated coverglass at 80% confluency and fixed on the following day for 5–10 min with MeOH at –20°C.

We generated HeLa T-Rex stable cell lines that expressed a siRNA-resistant C-term LAP-tagged Ndel1 WT, S285A or S285D variants behind a doxycycline inducible promoter as in Matson and Stukenberg (2014). Cells were cultured at 37°C in DMEM media (Life Technologies) supplemented with 10% FBS, 1 mM sodium pyruvate, 100 IU/ml penicillin, and 100 µg/ml streptomycin (Invitrogen). After transfection (36 h) with siRNA targeting, endogenous Ndel1 cells (Ndel1siResFW: AGGAATTTTGCAAAGGATCAGGCATCAC-GAAAATCCTATATTTCAGGG, Ndel1siResRV; CCCTGAAATATAG-GATTTTCGTGATGCCTGATCCTTTGCAAAATTCCT) were plated on acid-washed *poly*-lysine or fibronectin (Sigma) -coated coverglass and the expression of Ndel1 mutants was induced by the addition of 50 nM doxycyclin. Cells were fixed after an additional 36 h for 10–20 min with 2% paraformaldehyde (PFA) in PHEM buffer (60 mM PIPES, 25 mM HEPES, 10 mM EGTA, 2 mM MgCl2, pH 6.8) supplemented with 0.5% NP-40. AZD1152, MLN8054, or VX680 was added for 30 min before fixation at the specified concentrations to inhibit Aurora B kinase, Aurora A kinase, or both Aurora kinases, respectively.

For the experiment depicted in Figure 1, E and F, HeLa T-Rex cells were grown on acid-washed *poly*-lysine–coated coverglass and transfected at 60–80% confluency with plasmids carrying GFP or GFP-CC1 dynactin fragment. After 24 h, cells were treated with 1.5 µM MLN8054 for 30 min, followed by fixation with 2% PFA in PHEM buffer supplemented with 0.5% NP-40.

Live-cell imaging

Following knockdown of endogenous Ndel1 and expression of Ndel1 mutants in HeLa cells as described above, cells were treated with 20 nM nocodazole in the presence of 100 nM SiR-DNA dye and observed under a Zeiss Axiovert epifluorescent microscope using 10× objective in a 37°C chamber and 5% CO_2. Images were taken every 5 min for the period of 24 h. Quantification of the duration of mitosis was performed manually based on the DNA staining and brightfield images. Only the cells that entered mitosis within the first 12 h from the start of the imaging were taken into consideration.

Cell proliferation assay

Cells that were treated with siNdel1 and doxycyclin to induce Ndel1 expression were subsequently treated with 20 nM nocodazole, similarly as described above (see *Live-cell imaging*). A 5 × 5 grid of images was collected at the center of each well every 24 h using a Zeiss Axiovert microscope with 10× objective. Images were subsequently processed in ImageJ (Schneider *et al.*, 2012), image background and shading correction was done using the BaSiC plugin (Peng *et al.*, 2017), and confluence was quantified using the PHANTAST plugin (Jaccard *et al.*, 2014). Results were normalized to the confluence on day 0.
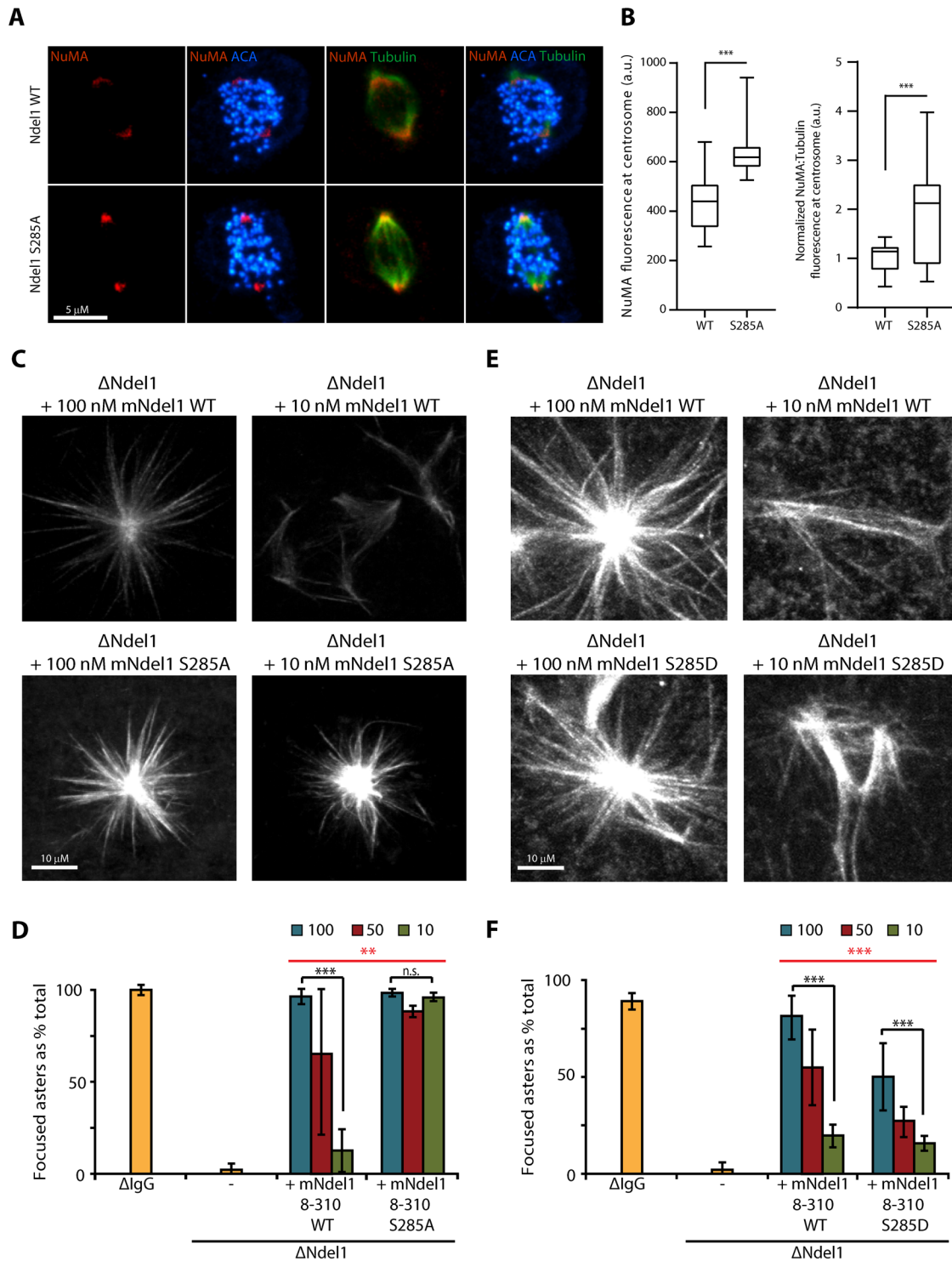
FIGURE 4: Phosphorylation of Ndel1 on Ser285 also limits the localization of NuMA to spindle poles and negatively regulates dynein-dependent aster formation in *Xenopus* egg extracts. (A, B) A nonphosphorylatable mutant of Ndel1 allows for increased recruitment of NuMA to the centrosomal region. (A) Representative images depicting localization of NuMA (red) in HeLa T-Rex cells expressing Ndel1 WT or Ndel1 S285A mutant in mitotic cells; bar = 5 μm. (B) Quantification of experiment depicted in panel A ($n = 20$ centrosomal regions; Student's t test, with ***, $p < 0.0005$). (C, D) A nonphosphorylatable mutant of Ndel1 generates Ran asters at lower concentrations than WT Ndel1. *Xenopus* egg extracts were depleted of Ndel1 and rescued with the indicated concentrations of recombinant mNdel1. Note that Ndel1 S285A mutant rescued aster formation at 10 nM (10-fold less than endogenous Ndel1 level), whereas the WT protein mNdel1$^{8–310}$ required higher concentrations to generate Ran asters. Representative microtubule structures are shown in panel C, bar = 10 μm, and the quantification is shown in panel D ($n > 100$ microtubule structures; $N = 3$; Student's t test, with *, $p < 0.05$; **, $p < 0.005$; ***, $p < 0.0005$; two-way ANOVA [red], with **, $p < 0.005$). (E, F) A phosphomimetic mutant of Ser285 is deficient in Ran aster formation in *Xenopus* egg extracts. Experiment was

Immunofluorescence

Fixed HeLa cells were blocked with 3% bovine serum albumin (BSA) in TBST (3% BSA/TBST), incubated with primary antibodies diluted in 3% BSA/TBST for 1 h, and washed three times with TBST. This was followed by a 30-min incubation with secondary antibodies diluted in 3% BSA/TBST and three washes with TBST. Cells were briefly incubated with 0.5 μg/ml 4′-6-diamidino-2-phenylindole (DAPI; Cell Signaling) diluted in water and mounted in ProLongGold medium (Invitrogen). Immunofluorescence on *Xenopus* S3 cells was performed similarly, with the exception that the primary antibodies were directly conjugated to fluorophores to enable three colors with two species. Cells were blocked with 3% BSA/TBST and 10% normal mouse serum or normal rabbit serum (both from Jackson Immunoresearch), followed by incubation with directly conjugated mouse (tubulin) or rabbit (Ndel1, p.Ndel1, Ndc80) antibodies, respectively. Primary antibodies were used at the following concentrations: anti-centromere (ACA; 1:500; Antibodies), anti-Ndel1 (1:100; Zyłkiewicz *et al.*, 2011), anti-pS285 (1:100; this study), anti-α-tubulin (1:200; Thermo), anti-α-tubulin-FITC (1:200; Sigma), anti-Mad1 (1:1000; Matson and Stukenberg, 2014), anti-NuMA (1:100; Cell Signaling), and anti-Ndc80 (1:200; Emanuele *et al.*, 2005). Secondary antibodies were purchased from Jackson Immunoresearch.

Microscopy

Imaging for experiments depicted in Figure 1E, Figure 2, Figure 3, Figure 4, and Supplemental Figure S2 was performed using a spinning-disk confocal imaging system with a 63× 1.4 NA Plan-Apochromatic Zeiss objective lens on a Zeiss Axiovert 200 inverted microscope. NanoScan Z motor (Prior), confocal attachment (Perkin Elmer), and a krypton/argon laser (Perkin Elmer) with acousto-optic-tunable filter were used to detect illumination at 488, 568, or 647 nm. Digital images were obtained with a digital CCD camera (Hamamatsu). Image acquisition, shutters, and z-slices were all controlled by Volocity imaging software (Perkin Elmer) on a Mac computer. Z-series optical overlapping sections were obtained in 0.4-μm steps. All images compared with each other were processed identically in Volocity (Perkin Elmer) to adjust contrast.

Experiments depicted in Figure 1, A and B, and Supplemental Figure S1 were imaged using a Zeiss LSM 880 scanning confocal microscope with a 63× NA Plan-Apochromatic Zeiss objective lens. A 32-channel GaAsP detector array was used for signal detection. Image acquisition, shutters, and z-slices were all controlled by Zen Black software (Zeiss) on a PC computer. Z-series optical overlapping sections were obtained in 0.5-μm steps.

Image analysis and quantification

Image analysis and quantification of fluorescence experiments were performed in Volocity (Perkin Elmer). To quantify the intensity at spindle poles, circular regions of interest (ROI) of diameter ~2 μm were drawn around areas of spindle pole signal as identified by microtubule staining. ROI areas were also drawn on blank regions for each cell analyzed to determine background intensity. Background intensity was calculated per volume unit (mm³) and subtracted from sum intensity/mm³ to directly compare background-corrected intensity/volume units between spindle poles with different volumes. Intensities were quantified separately for

each pole for 16–20 poles per condition and normalized to the mean of intensities at spindle poles in Ndel1 WT cells. The kinetochore localization of Mad1 was quantified semiautomatically in Volocity imaging software using ACA mask. Background intensity was calculated per volume unit (mm³) and subtracted from sum intensity/mm³ to directly compare background-corrected (normalized) intensity/volume units between kinetochores with different volumes. Intensities were quantified for >300 kinetochores from at least eight cells per condition. All quantified data are representative of a single experiment that has been replicated at least three times with similar trends.

Quantification of Figure 1, E and F, was performed by manual identification of cells. Centrosomal staining was defined as two strong Mad1 foci that were outside DNA identified by DAPI, which were easy to distinguish from cells that only had scattered foci (that colocalized with ACA) and are within the DAPI mass.

Cloning and protein purification

Constructs of mNdel1 were prepared as previously described (Zyłkiewicz *et al.*, 2011). Briefly, PCR-amplified Ndel1 fragments were ligated into pHis-Parallel2 vector (Sheffield *et al.*, 1999) via NcoI and NdeI restrictive sites to yield an N-terminally tagged mNdel1 variant 8–192, and C-terminally tagged mNdel1 8–310 and 191–250. 6-His-tagged proteins were expressed in the *Escherichia coli* strain BL21 (DE3/RIPL; Stratagene), and purified using Ni-NTA resin (Qiagen) and gel filtration over Superdex 200 (Amersham Biosciences). Mutations were introduced using a site-directed mutagenesis kit (Qiagen) and were verified by sequencing. For rescue experiments proteins were dialyzed into 10 mM K-HEPES, 100 mM KCl, pH 7.2.

Kinase assays

Kinase assays were performed in 100-μl reaction volumes containing 100 μg of Ndel1 proteins (mNdel1$^{8-192}$, mNdel1$^{191-250}$, or mNdel1$^{8-310}$), 1× kinase buffer (20 mM Tris, pH 7.5, 1 mM MgCl2, 25 mM KCl, 1 mM dithiothreitol [DTT], 40 μg/ml BSA), 100 μM ATP, 0.3 μl of 5 mCi/ml γ-^{32}P-ATP, and 2 μl of kinase. The following kinases were used: Aurora A (Satinover *et al.*, 2004) and Aurora B (NEB).

Mass spectrometry

In vitro Aurora B-INCENP$^{790-847}$ (Sessa *et al.*, 2005) phosphorylated Ndel1(8–310) protein was reduced with DTT, alkylated with iodo-acetamide and digested with 1 μg of modified trypsin (Promega) overnight at room temperature. The sample was acidified to 5% acetic acid and the resulting peptides were identified at the Mass Spectrometry Core Facility at the University of Virginia using an LC-MS/MS system consisting of a Thermo Electron LTQFT mass spectrometer and a Protana nanospray ion source interfaced to a self-packed 8 cm × 75 μm id Phenomenex Jupiter 10 μm C18 reversed-phase capillary column. The sample (20%) was injected into the instrument, and peptides were eluted from the column by an acetonitrile/0.1 M acetic acid gradient at a flow rate of 0.4 μl/min over 1 h. The nanospray ion source was operated at 2.8 kV. The instrument was set to collect in a data-dependent manner with a MS scan (FT-resolution 100K) followed by MS/MS on the top 10 ions (IT–CID). A similar MS run was done on a Thermo Electron LTQXL using ETD fragmentation to provide complimentary data.

---

performed as in panels C and D, except the Ndel1 S285D mutant was used. Note that at endogenous concentrations of 100 nM the S285D mutant did not rescue aster formation. Representative microtubule structures are shown in panel E (bar = 10 μm) and the quantification is shown in panel F ($n > 100$ microtubule structures; $N = 3$; Student's *t* test, with *, $p < 0.05$; **, $p < 0.005$; ***, $p < 0.0005$; two-way ANOVA [red], with ***, $p < 0.0005$).

Identification of phosphorylated peptides

Data from the LTQFT was searched against the complete protein sequence of Ndel1 using the Sequest algorithm within Thermo Electron Bioworks 3.3.1 with a parent tolerance of 10 ppm and a fragment tolerance of 0.8 Da allowing for a fixed modification to C (carbamidomethyl) and variable modifications to M (oxidation) and STY (phosphorylation). General Xcorr and peptide prophet filters were used through Scaffold (Proteome Software v 1.7.0) to generate a list of possible peptides from Ndel1. Those peptides that were potentially phosphorylated were examined manually using CID and ETD spectra to determine the site of phosphorylation (in one case only narrowed to a region). The list of phosphosites was then used in comparison to predicted sites/kinases and domains within Ndel1 to determine sites of interest for further study.

Xenopus egg extract experiments

Depletion and rescue experiments were performed and quantified as previously described (Zyłkiewicz *et al.*, 2011). Titration experiments were repeated three times and at least 100 microtubule structures were quantified for each condition as previously described (Zyłkiewicz *et al.*, 2011). Counting was done blind and similarly localized areas were picked for each sample.

REFERENCES

Auckland P, Roscioli E, Coker HLE, McAinsh AD (2020). CENP-F stabilizes kinetochore-microtubule attachments and limits dynein stripping of corona cargoes. J Cell Biol 219, e201905018.

Barr AR, Gergely F (2007). Aurora-A: the maker and breaker of spindle poles. J Cell Sci 120, 2987–2996.

Bradshaw NJ, Soares DC, Carlyle BC, Ogawa F, Davidson-Smith H, Christie S, Mackie S, Thomson PA, Porteous DJ, Millar JK (2011). PKA phosphorylation of NDE1 is DISC1/PDE4 dependent and modulates its interaction with LIS1 and NDEL1. J Neurosci 31, 9043–9054.

Carmena M, Earnshaw WC (2003). The cellular geography of Aurora kinases. Nat Rev Mol Cell Biol 4, 842–854.

Chinen T, Yamamoto S, Takeda Y, Watanabe K, Kuroki K, Hashimoto K, Takao D, Kitagawa D (2020). NuMA assemblies organize microtubule asters to establish spindle bipolarity in acentrosomal human cells. EMBO J 39, e102378.

Chmátal L, Yang K, Schultz R M, Lampson M A (2015). Spatial regulation of kinetochore microtubule attachments by destabilization at spindle poles in meiosis I. Curr Biol 25, 1835–1841.

de Groot CO, Hsia JE, Anzola JV, Motamedi A, Yoon M, Wong YL, Jenkins D, Lee HJ, Martinez MB, Davis RL, *et al.* (2015). A cell biologist's field guide to aurora kinase inhibitors. Front Oncol 5, 285.

DeLuca KF, Meppelink A, Broad AJ, Mick JE, Peersen OB, Pektas S, Lens SMA, DeLuca JG (2018a). Aurora A kinase phosphorylates Hec1 to regulate metaphase kinetochore-microtubule dynamics. J Cell Biol 217, 163–177.

DeLuca K F, Meppelink A, Broad A J, Mick J E, Peersen O B, Pektas S, Lens S M A, DeLuca J G (2018b). Aurora A kinase phosphorylates Hec1 to regulate metaphase kinetochore–microtubule dynamics. J Cell Biol 217, 163–177.

Derewenda U, Tarricone C, Choi WC, Cooper DR, Lukasik S, Perrina F, Tripathy A, Kim MH, Cafiso DS, Musacchio A, Derewenda ZS (2007). The structure of the coiled-coil domain of Ndel1 and the basis of its interaction with Lis1, the causal protein of Miller-Dieker lissencephaly. Structure 15, 1467–1481.

Dionne MA, Howard L, Compton DA (1999). NuMA is a component of an insoluble matrix at mitotic spindle poles. Cell Motil Cytoskeleton 42, 189–203.

Ditchfield C, Johnson VL, Tighe A, Ellston R, Haworth C, Johnson T, Mortlock A, Keen N, Taylor SS (2003). Aurora B couples chromosome alignment with anaphase by targeting BubR1, Mad2, and Cenp-E to kinetochores. J Cell Biol 161, 267–280.

Efimov VP, Morris NR (2000). The LIS1-related NUDF protein of *Aspergillus nidulans* interacts with the coiled-coil domain of the NUDE/RO11 protein. J Cell Biol 150, 681–688.

Emanuele MJ, McCleland ML, Satinover DL, Stukenberg PT (2005). Measuring the stoichiometry and physical interactions between components elucidates the architecture of the vertebrate kinetochore. Mol Biol Cell 16, 4882–4892.

Eot-Houllier G, Magnaghi-Jaulin L, Fulcrand G, Moyroud F-X, Monier S, Jaulin C (2018). Aurora A-dependent CENP-A phosphorylation at inner centromeres protects bioriented chromosomes against cohesion fatigue. Nat Commun 9, 1888.

Fuller BG, Lampson MA, Foley EA, Rosasco-Nitcher S, Le KV, Tobelmann P, Brautigan DL, Stukenberg PT, Kapoor TM (2008). Midzone activation of aurora B in anaphase produces an intracellular phosphorylation gradient. Nature 453, 1132–1136.

Gaglio T, Saredi A, Compton DA (1995). NuMA is required for the organization of microtubules into aster-like mitotic arrays. J Cell Biol 131, 693–708.

Gallini S, Carminati M, De Mattia F, Pirovano L, Martini E, Oldani A, Asteriti IA, Guarguaglini G, Mapelli M (2016). NuMA phosphorylation by Aurora-A orchestrates spindle orientation. Curr Biol 26, 458–469.

Gassmann R, Holland AJ, Varma D, Wan X, Filiz C, Oegema K, Salmon ED, Desai A (2010). Removal of Spindly from microtubule-attached kinetochores controls spindle checkpoint silencing in human cells. Genes Dev 24, 957–971.

Giet R, McLean D, Descamps S, Lee MJ, Raff JW, Prigent C, Glover DM (2002). *Drosophila* Aurora A kinase is required to localize D-TACC to centrosomes and to regulate astral microtubules. J Cell Biol 156, 437–451.

Giet R, Prigent C (2000). The *Xenopus laevis* aurora/Ip11p-related kinase pEg2 participates in the stability of the bipolar mitotic spindle. Exp Cell Res 258, 145–151.

Gopalan G, Chan CSM, Donovan PJ (1997). A novel mammalian, mitotic spindle-associated kinase is related to yeast and fly chromosome segregation regulators. J Cell Biol 138, 643–656.

Harrington EA, Bebbington D, Moore J, Rasmussen RK, Ajose-Adeogun AO, Nakayama T, Graham JA, Demur C, Hercend T, Diu-Hercend A, *et al.* (2004). VX-680, a potent and selective small-molecule inhibitor of the Aurora kinases, suppresses tumor growth in vivo. Nat Med 10, 262–267.

Heald R, Tournebize R, Blank T, Sandaltzopoulos R, Becker P, Hyman A, Karsenti E (1996). Self-organization of microtubules into bipolar spindles around artificial chromosomes in *Xenopus* egg extracts. Nature 382, 420–425.

Hebbar S, Mesngon MT, Guillotte AM, Desai B, Ayala R, Smith DS (2008). Lis1 and Ndel1 influence the timing of nuclear envelope breakdown in neural stem cells. J Cell Biol 182, 1063–1071.

Howell BJJ, McEwen BFF, Canman JCC, Hoffman DBB, Farrar EMM, Rieder CLL, Salmon EDD (2001). Cytoplasmic dynein/dynactin drives kinetochore protein transport to the spindle poles and has a role in mitotic spindle checkpoint inactivation. J Cell Biol 155, 1159–1172.

Huang J, Roberts AJ, Leschziner AE, Reck-Peterson SL (2012). Lis1 acts as a "clutch" between the ATPase and microtubule-binding domains of the dynein motor. Cell 150, 975–986.

Jaccard N, Griffin LD, Keser A, Macown RJ, Super A, Veraitch FS, Szita N (2014). Automated method for the rapid and precise estimation of adherent cell culture characteristics from phase contrast microscopy images. Biotechnol Bioeng 111, 504–517.

Kamiya A, Tomoda T, Chang J, Takaki M, Zhan C, Morita M, Cascio MB, Elashvili S, Koizumi H, Takanezawa Y, *et al.* (2006). DISC1-NDEL1/ NUDEL protein interaction, an essential component for neurite outgrowth, is modulated by genetic variations of DISC1. Hum Mol Genet 15, 3313–3323.

Katayama H, Sasai K, Kloc M, Brinkley BR, Sen S (2008). Aurora kinase-A regulates kinetochore/chromatin associated microtubule assembly in human cells. Cell Cycle 7, 2691–2704.

King JM, Hays TS, Nicklas RB (2000). Dynein is a transient kinetochore component whose binding is regulated by microtubule attachment, not tension. J Cell Biol 151, 739–748.

Kiyomitsu T, Boerner S (2021). The Nuclear Mitotic Apparatus (NuMA) Protein: A Key Player for Nuclear Formation, Spindle Assembly, and Spindle Positioning. Front Cell Dev Biol 9, https://doi.org/10.3389/fcell.2021.653801.

Mangal S, Sacher J, Kim T, Osório DS, Motegi F, Carvalho AX, Oegema K, Zanin E (2018). TPXL-1 activates Aurora A to clear contractile ring components from the polar cortex during cytokinesis. J Cell Biol 217, 837–848.

Matson DR, Stukenberg PT (2014). CENP-I and Aurora B act as a molecular switch that ties RZZ/Mad1 recruitment to kinetochore attachment status. J Cell Biol 205, 541–554.

McKenney RJ, Vershinin M, Kunwar A, Vallee RB, Gross SP (2010). LIS1 and NudE induce a persistent dynein force-producing state. Cell 141, 304–314.

Merdes A, Heald R, Samejima K, Earnshaw WC, Cleveland DW (2000). Formation of spindle poles by dynein/dynactin-dependent transport of NuMA. J Cell Biol 149, 851–862.

Merdes A, Ramyar K, Vechio JD, Cleveland DW (1996). A complex of NuMA and cytoplasmic dynein is essential for mitotic spindle assembly. Cell 87, 447–458.

Mori D, Yano Y, Toyo-oka K, Yoshida N, Yamada M, Muramatsu M, Zhang D, Saya H, Toyoshima YY, Kinoshita K, et al. (2007). NDEL1 phosphorylation by Aurora-A kinase is essential for centrosomal maturation, separation, and TACC3 recruitment. Mol Cell Biol 27, 352–367.

Mori D, Yamada M, Mimori-Kiyosue Y, Shirai Y, Suzuki A, Ohno S, Saya H, Wynshaw-Boris A, Hirotsune S (2009). An essential role of the aPKC-Aurora A-NDEL1 pathway in neurite elongation by modulation of microtubule dynamics. Nat Cell Biol 11, 1057–1068.

Nyarko A, Song Y, Barbar E (2012). Intrinsic disorder in dynein intermediate chain modulates its interactions with NudE and dynactin. J Biol Chem 287, 24884–24893.

Peng T, Thorn K, Schroeder T, Wang L, Theis FJ, Marr C, Navab N (2017). A BaSiC tool for background and shading correction of optical microscopy images. Nat Commun 8, 1–7.

Quintyne NJ, Gill SR, Eckley DM, Crego CL, Compton DA, Schroer TA (1999). Dynactin is required for microtubule anchoring at centrosomes. J Cell Biol 147, 321–334.

Reck-Peterson SL, Redwine WB, Vale RD, Carter AP (2018). The cytoplasmic dynein transport machinery and its many cargoes. Nat Rev Mol Cell Biol 19, 382–398.

Satinover DL, Leach CA, Stukenberg PT, Brautigan DL (2004). Activation of Aurora-A kinase by protein phosphatase inhibitor-2, a bifunctional signaling protein. Proc Natl Acad Sci USA 101, 8625–8630.

Schneider CA, Rasband WS, Eliceiri KW (2012). NIH Image to ImageJ: 25 years of image analysis. Nat Methods 9, 671–675.

Seldin L, Muroyama A, Lechler T (2016). NuMA-microtubule interactions are critical for spindle orientation and the morphogenesis of diverse epidermal structures. Elife 5, e12504.

Sessa F, Mapelli M, Ciferri C, Tarricone C, Areces LB, Schneider TR, Stukenberg PT, Musacchio A (2005). Mechanism of Aurora B activation by INCENP and inhibition by hesperadin. Mol Cell 8, 379–391.

Sheffield P, Garrard S, Derewenda Z (1999). Overcoming expression and purification problems of RhoGDI using a family of "parallel" expression vectors. Protein Expr Purif 15, 34–39.

Silk AD, Holland AJ, Cleveland DW (2009). Requirements for NuMA in maintenance and establishment of mammalian spindle poles. J Cell Biol 184, 677–690.

Stehman SA, Chen Y, McKenney RJ, Vallee RB (2007). NudE and NudEL are required for mitotic progression and are involved in dynein recruitment to kinetochores. J Cell Biol 178, 583–594.

Takitoh T, Kumamoto K, Wang CC, Sato M, Toba S, Wynshaw-Boris A, Hirotsune S (2012). Activation of Aurora-A is essential for neuronal migration via modulation of microtubule organization. J Neurosci 32, 11050–11066.

Vaisberg EA, Koonce MP, McIntosh JR (1993). Cytoplasmic dynein plays a role in mammalian mitotic spindle formation. J Cell Biol 23, 849–858.

Wang E, Ballister ER, Lampson MA (2011). Aurora B dynamics at centromeres create a diffusion-based phosphorylation gradient. J Cell Biol 194, 539–549.

Wang S, Zheng Y (2011). Identification of a novel dynein binding domain in nudel essential for spindle pole organization in Xenopus egg extract. J Biol Chem 286, 587–593.

Wiese C, Wilde A, Moore MS, Adam SA, Merdes A, Zheng Y (2001). Role of importin-β in coupling ran to downstream targets in microtubule assembly. Science 291, 653–656.

Wynne CL, Vallee RB (2018). Cdk1 phosphorylation of the dynein adapter Nde1 controls cargo binding from G2 to anaphase. J Cell Biol 217, 3019–3029.

Ye AA, Deretic J, Hoel CM, Hinman AW, Cimini D, Welburn JP, Maresca TJ (2015). Aurora A kinase contributes to a pole-based error correction pathway. Curr Biol 25, 1842–1851.

Ye F, Kang E, Yu C, Qian X, Jacob F, Yu C, Mao M, Poon RYC, Kim J, Song H, et al. (2017). DISC1 Regulates Neurogenesis via Modulating Kinetochore Attachment of Ndel1/Nde1 during Mitosis. Neuron 96, 1041–1054.e5.

Yeh TY, Peretti D, Chuang JZ, Rodriguez-Boulan E, Sung CH (2006). Regulatory dissociation of Tctex-1 light chain from dynein complex is essential for the apical delivery of rhodopsin. Traffic 7, 1495–1502.

Zyłkiewicz E, Kijańska M, Choi WC, Derewenda U, Derewenda ZS, Stukenberg PT (2011). The N-terminal coiled-coil of Ndel1 is a regulated scaffold that recruits LIS1 to dynein. J Cell Biol 192, 433–445.